Program Digest, 2019 IEEE International Ultrasonics Symposium (IUS)
Glasgow, Scotland, October 6-9, 2019

Three-dimensional Super-Resolution Ultrasound Microvessel Imaging with Bipartite Graph-based Microbubble Tracking using a Verasonics 256-channel Ultrasound System

U-Wai Lok[1], Chengwu Huang[1], Shanshan Tang[1], Ping Gong[1], Fabrice Lucien[2], Yohan Kim[2], Pengfei Song[1,3,4], and Shigao Chen[1]
[1]Department of Radiology, Mayo Clinic College of Medicine and Science, Rochester, MN
[2]Department of Urology, Mayo Clinic College of Medicine and Science, Mayo Clinic, Rochester, MN
[3]Beckman Institute, University of Illinois at Urbana-Champaign, Urbana, IL
[4]Department of Electrical and Computer Engineering, University of Illinois at Urbana-Champaign, Urbana, IL

Abstract*– Three-dimensional (3-D) super-resolution ultrasound microvessel imaging (SR-UMI) has been recently proposed to visualize 3-D microvasculature by overcoming the diffraction limited resolution in three spatial dimensions. However, 3-D SR-UMI suffers from high system complexity and sophisticated microbubble tracking mechanisms to account for 3D movement. To reduce the system complexity, methods such as row-column matrix, sparse array and micro-beamforming have been proposed to reduce the number of transmit/receive channel at the cost of degradation of image quality. In this study, a sub-aperture process is used to reduce the required received channel counts at the cost of slightly reducing the overall frame rate. For the microbubble tracking, two dimensional (2-D) bipartite graph-based tracking has been proposed to improve microbubble tracking performance for 2-D SR-UMI. This approach can reduce the background noise, improve the performance of super-resolution image, and stabilize the estimated micro-vessel flow speed. We extended the 2-D bipartite graph-based method to 3-D SR-UMI to reduce background noise and to improve the micro-bubble tracking performance. In this study, a flow channel phantom was used to evaluate the performance of the proposed method. Results showed that the proposed method can effectively improve the spatial resolution as compared with 3-D Power Doppler images.

Keywords— Super-resolution ultrasound microvessel imaging, compensation, 3-D bipartite graph-based method

I. Introduction

Two-dimensional (2-D) microbubble-based super-resolution ultrasound microvessel imaging (SR-UMI) has been proposed which can highly improve the spatial resolution in the previous studies [1-4]. The basic concept of the super-resolution imaging is to localize the center positions of the micro-bubbles and track the movement of the micro-bubbles to estimate the micro-vessel flow speed [5-6]. However, to prompt SR-UMI from 2-D to 3-D remains challenging due to the high system complexity and the demand of the sophisticated micro-bubble tracking.

For a 3-D super-resolution ultrasound microvessel imaging (3-D SR-UMI) system, a 2-D matrix array probe is used in this study. The advantage of using a 2D matrix probe is that it allows two-dimensional dynamic focusing on both lateral and elevational directions, and thus, no exhaustive scanning is needed. However, a fully sampled 2-D array usually consists of thousands of channels, thus, high system complexity is required.

To achieve high quality of 3-D SR-UMI with fewer channels, various approaches have been investigated to achieve required ultrasound data such as sub-aperture process, sparse array, row column matrix and micro-beamforming. Despite the system complexity is reduced, the image quality is also degraded due to the reduction of channel counts. Therefore, in this study, we adopted the sub-aperture process to receive ultrasound RF data to perform 3-D SR-UMI. In this study, 1024 channel-system was used to transmit ultrasound plane wave signals with a specified steered angle, and then four apertures were used to receive the ultrasound RF data. Each aperture consists of 256 channels (8×32 channels, where the number of channels in lateral and elevational directions are 8 channels and 32 channels, respectively) to receive the ultrasound RF data. 1024 channel data can be obtained when all 4 sub-aperture data were captured, resulting in 4-fold reduction for the system complexity at the cost of reducing frame rate.

On the other hand, micro-bubble tracking in 3-D is crucial for the 3-D SR-UMI. In [5], Markov-chain-Monte-Carlo method has been proposed for the 2-D SR-UMI, however, extremely high computational complexity is required to find the trajectories micro-bubble signals in a 3-D volume. Previously, we proposed a 2-D bipartite graph-based pairing approach [7] to improve the tracking performance. It can be easily performed by tracking microbubbles between two consecutive frames at a time. A micro-bubble is considered to be a valid micro-bubble as it can be paired within several frames and this approach is suitable to apply in a 3D environment, therefore, we extended the 2-D bipartite graph-based method to 3-D SR-UMI to reduce background noise and to improve the micro-bubble tracking performance.

The remainder of this paper is organized as follows: Section II provides the method and material to perform 3-D SR-UMI. Section III presents the results of the proposed method. Conclusions are drawn in Sections IV.

II. Method and Material

II-A) Data acquisition:

A Verasonics Vantage 256 channel ultrasound system was used with a 1024 channel 2-D matrix array (Vermon S.A., Tours, France, center frequency: 8MHz) which allows ultrasound signals to be transmitted for all 1024 channels and to be received for a 256 channel sub-aperture. 1024-channel ultrasound RF (radio-frequency) data can be achieved by switching between four sub-apertures. The received RF data acquired from 4 sub-apertures were then passed through 3-D receive beamforming using Verasonics' internal beamforming function. In-phase/Quadrature phase (IQ) data can be obtained after the receive beamforming process. Then the IQ data were saved for the subsequent data processes.

II-B) Clutter rejection:

The IQ data after receive beamforming were then passed through a clutter filter for tissue clutter rejection. Tissue backscatter signal reveals higher spatiotemporal coherence and power than blood signal, which can be conveniently separated from blood signals in the domain of singular-values. Tissue backscatter signal is typically projected in low order singular values after SVD process. Therefore, a 3-D SVD-based clutter filter was used for the tissue clutter rejection in this study. The low-order singular values were discarded to reject the tissue clutter.

II-C) 3-D microbubble localization:

After tissue clutter filtering, the filtered microbubble signals were normalized, interpolated and thresholded by an intensity value. Localization process was then applied to detect the center locations of microbubble signals. A system 3-D point spread function (PSF) was derived to perform 3-D normalized cross-correlation with the microbubbles signals. The centers of microbubbles were identified by searching for the peaks of 3-D normalized cross-correlation between a system 3-D point spread function and interpolated microbubble signals.

II-D) 3-D bipartite graph-based pairing approach:

After localization process, 3-D bipartite graph-based pairing approach was performed. Two microbubble signals in two consecutive frames were paired as the distances and velocities between them were acceptable. A detected microbubble was considered to be a reliable microbubble signal when it was paired in 10 consecutive frames. After that a linear interpolation was applied to the consecutively paired 10 steps microbubble trajectory to in-paint the gap between two microbubble locations.

II. Results

To evaluate the performance with and without the 3-D bipartite graph-based pairing approach (including pairing and interpolation), ultrasound IQ data were acquired from a flow channel phantom with a diameter of 1.4 mm. The syringe was attached to a motorized syringe pump (New Era Pump, N1000) to pump diluted micro-bubbles through the flow channel phantom with a constant flow velocity. The flow channel phantom was located in a water tank. The spatial resolution of each pixel was nearly 0.2 mm. After interpolation, the resolution of each pixel was nearly 0.02 mm. In this experiment, 4 angles (-4°, -2°, 0°, 2°) were used for compounding and the frame rate after compounding reached nearly 300 Hz. The transmit voltage was set as 20 V as well. The total number of frames used in this experiment was 2000 frames.

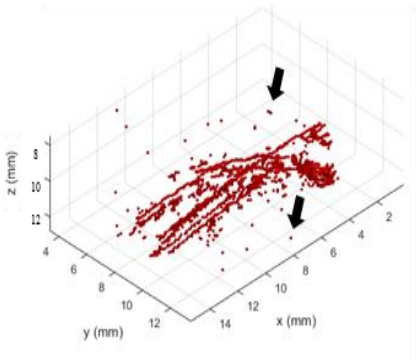

(a)

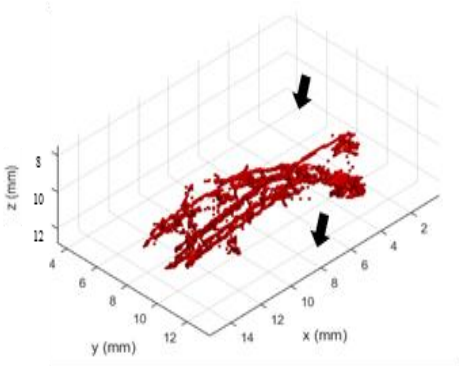

(b)

Fig. 1 Reconstructed images (a) without bipartition graph-based tracking and (b) bipartition graph-based tracking using 600 frames of data.

The image after localization using 600 frames is shown in Fig. 1 (a). Background noises are obviously observed as indicating in black arrows in Fig. 1 (a). The image using the 3-D bipartition graph-based pairing approach is shown in Fig. 1 (b).

As compared to Fig. 1 (a), background noise can be suppressed with the 3-D bipartition graph-based pairing approach. In addition, the image quality can be improved using 3-D interpolation after pairing.

The corresponding illustration photo of the flow channel phantom is shown in Fig. 2 (a). The region of interest is shown in the red dash box in the Fig. 2 (a). The reconstructed image using the proposed method is shown in Fig. 2 (b). It

should be noted that the image shown in the Fig. 2 (b) is the accumulation of 2000 frames using the proposed method. We can see that no background noises were observed after the proposed method.

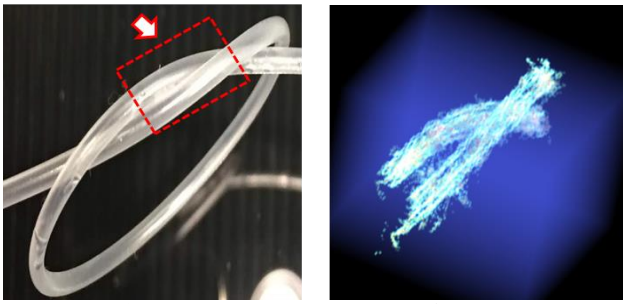

(a) (b)

Fig. 2. (a) An Illustration photo of the flow channel phantom (imaging region is denoted by the red dashed box), (b) the reconstructed 3D SR-UMI image of the flow channel phantom.

IV. Conclusions

In this study, we proposed the use of sub-aperture process to reduce the system complexity to maintain an acceptable image quality for subsequent microbubble localization and tracking. For the micro-bubble tracking process, we extended the 2-D bipartition graph-based pairing approach to the 3-D SR-UMI as well. The results showed that random background noise can be suppressed with the 3-D bipartition graph-based pairing approach. We also expected that the micro-bubble movement can also be tracked using this approach as well.

References

[1] C. Errico *et al.*, "Ultrafast ultrasound localization microscopy for deep super-resolution vascular imaging," *Nature,* vol. 527, p. 499, 11/25/online 2015.

[2] O. M. Viessmann, R. J. Eckersley, K. Christensen-Jeffries, M. X. Tang, and C. Dunsby, "Acoustic super-resolution with ultrasound and microbubbles," *Physics in Medicine & Biology,* vol. 58, no. 18, p. 6447, 2013.

[3] T. Opacic *et al.*, "Motion model ultrasound localization microscopy for preclinical and clinical multiparametric tumor characterization," *Nature Communications,* vol. 9, no. 1, p. 1527, 2018/04/18 2018.

[4] F. Lin, S. E. Shelton, D. Espíndola, J. D. Rojas, G. Pinton, and P. A. Dayton, "3-D Ultrasound Localization Microscopy for Identifying Microvascular Morphology Features of Tumor Angiogenesis at a Resolution Beyond the Diffraction Limit of Conventional Ultrasound," *Theranostics,* vol. 7, no. 1, pp. 196-204, 2017.

[5] K. Christensen-Jeffries, R. J. Browning, M. Tang, C. Dunsby, and R. J. Eckersley, "In Vivo Acoustic Super-Resolution and Super-Resolved Velocity Mapping Using Microbubbles," *IEEE Transactions on Medical Imaging,* vol. 34, no. 2, pp. 433-440, 2015.

[6] K. B. Hansen *et al.*, "Robust microbubble tracking for super resolution imaging in ultrasound," in *2016 IEEE International Ultrasonics Symposium (IUS)*, pp. 1-4, 2016.

[7] P. Song *et al.*, "Improved Super-Resolution Ultrasound Microvessel Imaging With Spatiotemporal Nonlocal Means Filtering and Bipartite Graph-Based Microbubble Tracking," *IEEE Transactions on Ultrasonics, Ferroelectrics, and Frequency Control,* vol. 65, no. 2, pp. 149-167, 2018.